Electronic Supplementary Material (ESI)

Supporting Information

Enhanced xenon adsorption and separation of anionic indium-oragnic framework by ion exchange with Co^{2+}

Bo-yu Liu, You-jin Gong, Xiao-nan Wu, Qiang Liu, Wei Li, Shun-shun Xiong*, Sheng Hu* and Xiao-lin Wang

Institute of Nuclear Physics and Chemistry, China Academy of Engineering Physics, Mianyang, Sichuan, 621900, P. R. China. E-mail: ssxiong@caep.cn, husheng205@caep.cn

Thermal stability

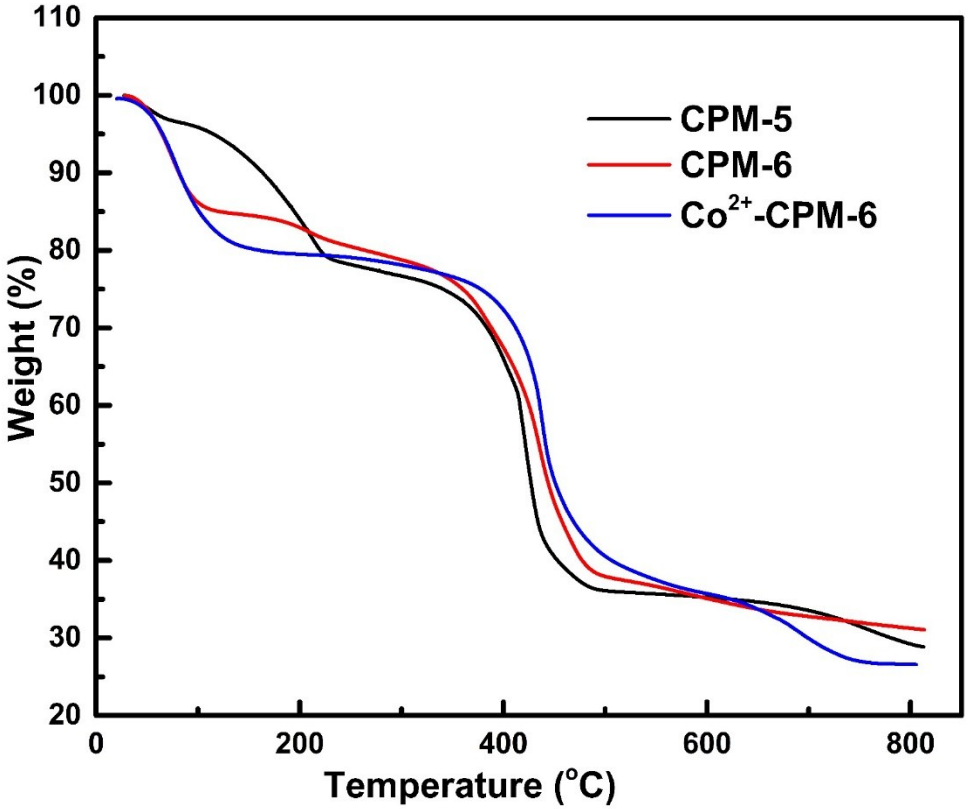

Figure S1. TGA curves of as-synthesized CPM-5, CPM-6 and Co^{2+}-CPM-6.

Pore size distribution

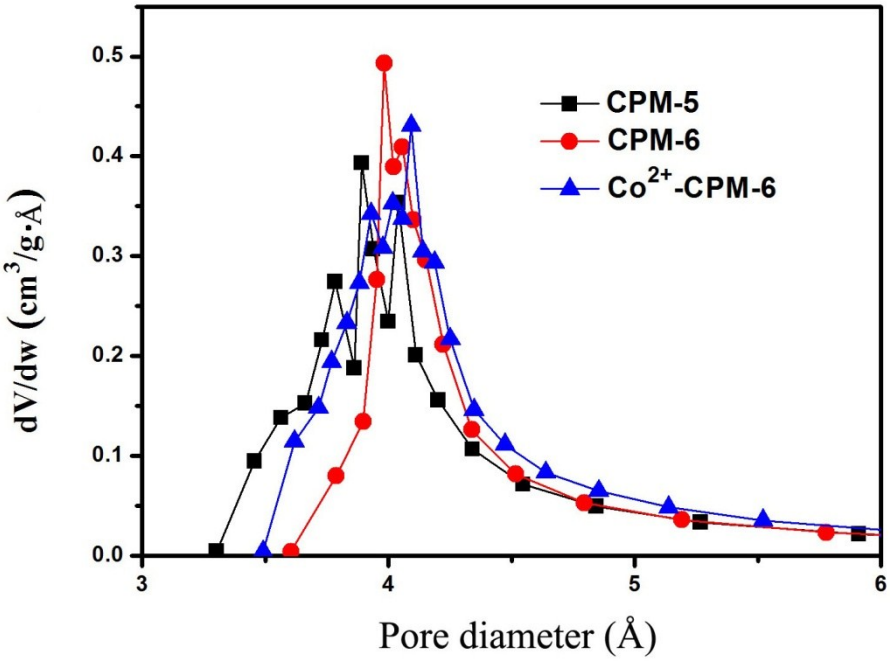

Figure S2. Pore size distribution for CPM-5, CPM-6 and Co^{2+}-CPM-6 using Horvath-Kawazoe Model.

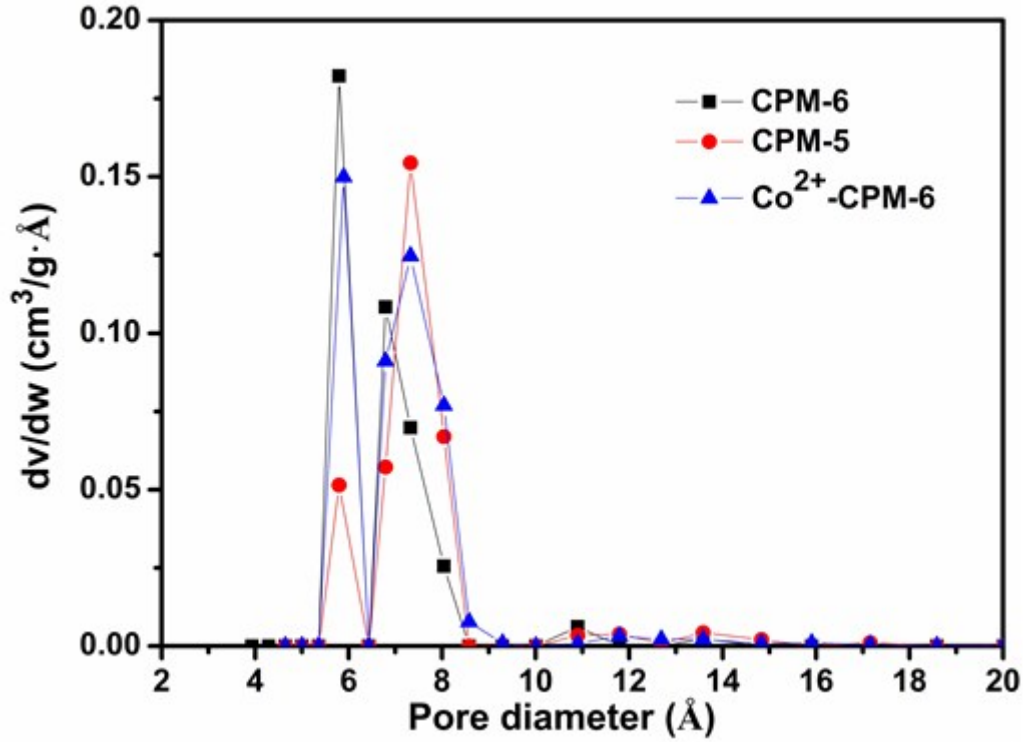

Figure S3. Pore size distribution for CPM-5, CPM-6 and Co^{2+}-CPM-6 using DFT model.

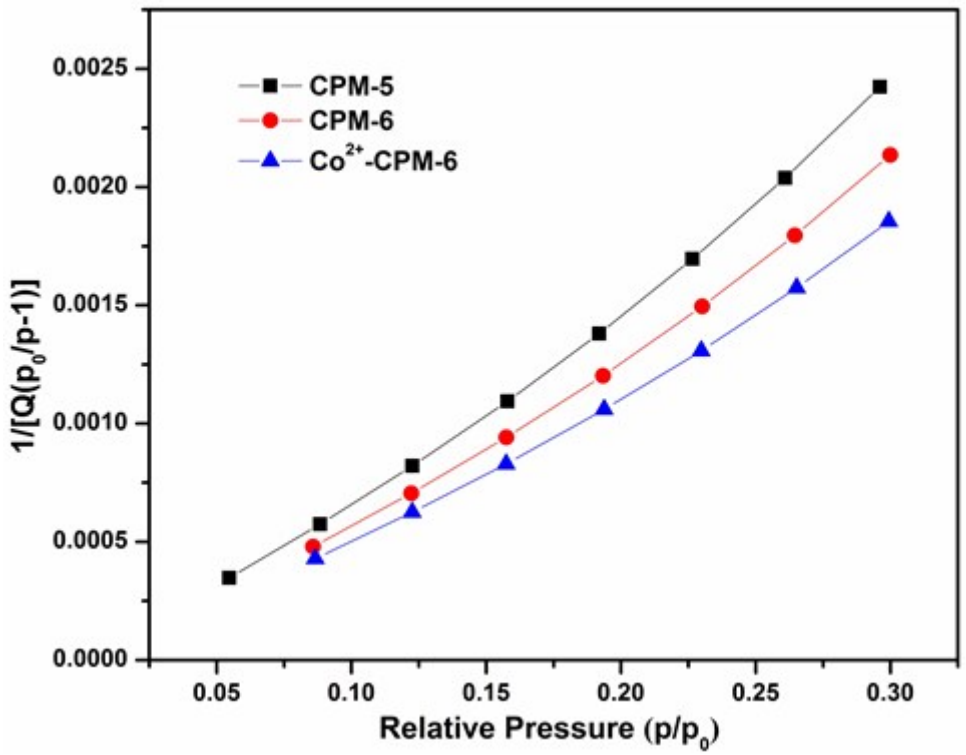

Figure S4. BET surface area plots for CPM-5, CPM-6 and Co^{2+}-CPM-6.

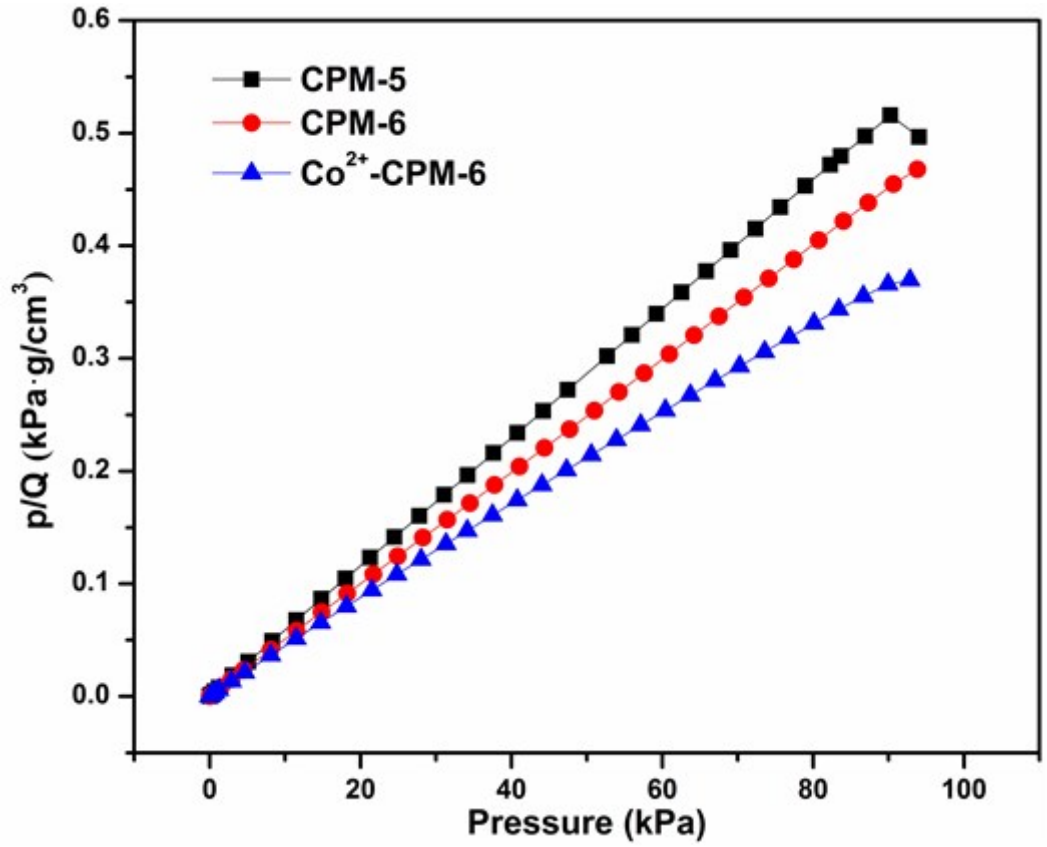

Figure S5. Langmuir surface area plots for CPM-5, CPM-6 and Co^{2+}-CPM-6.

Henry's constant fitting

The low range of the adsorption isotherm is nearly linear which corresponds to Henry's law behavior. The Henry's constants were obtained from a linear fit to the in low pressure part of the isotherm and the slope of the straight fitting line represents the corresponding Henry's constant.

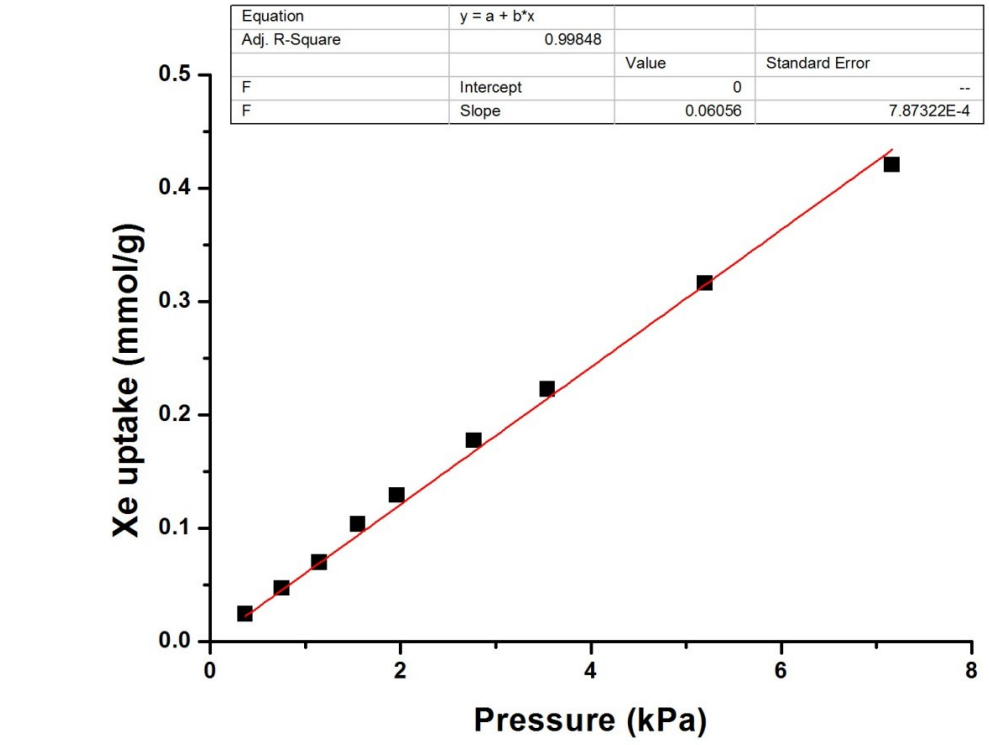

Figure S6. Henry coefficient fitting of Xe adsorption isotherm CPM-5 at 298K.

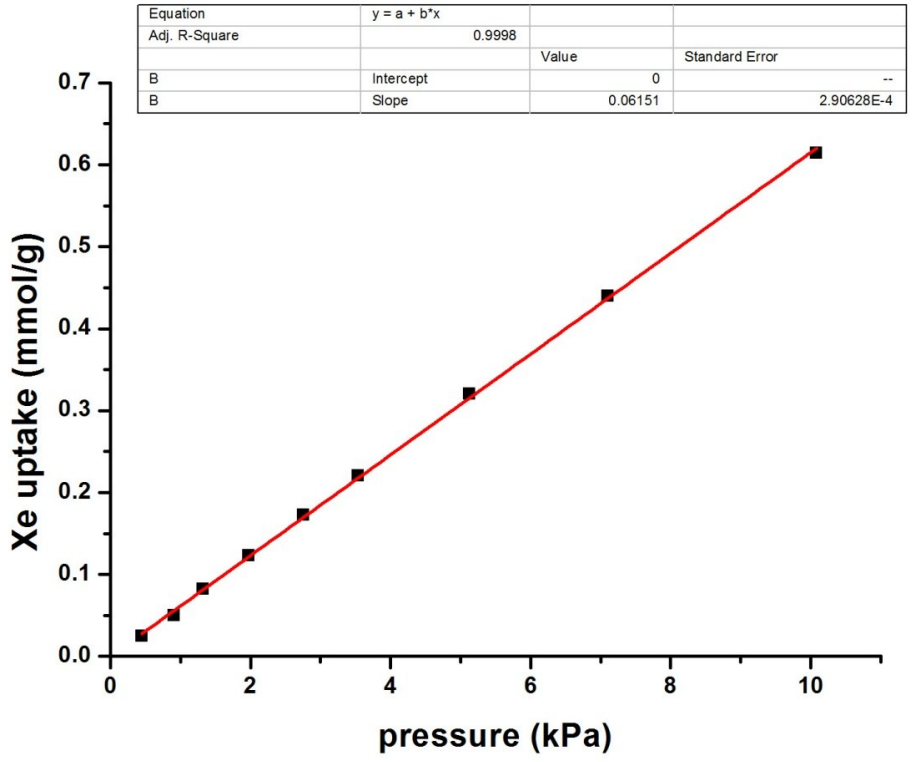

Figure S7. Henry coefficient fitting of Xe adsorption isotherm CPM-6 at 298K.

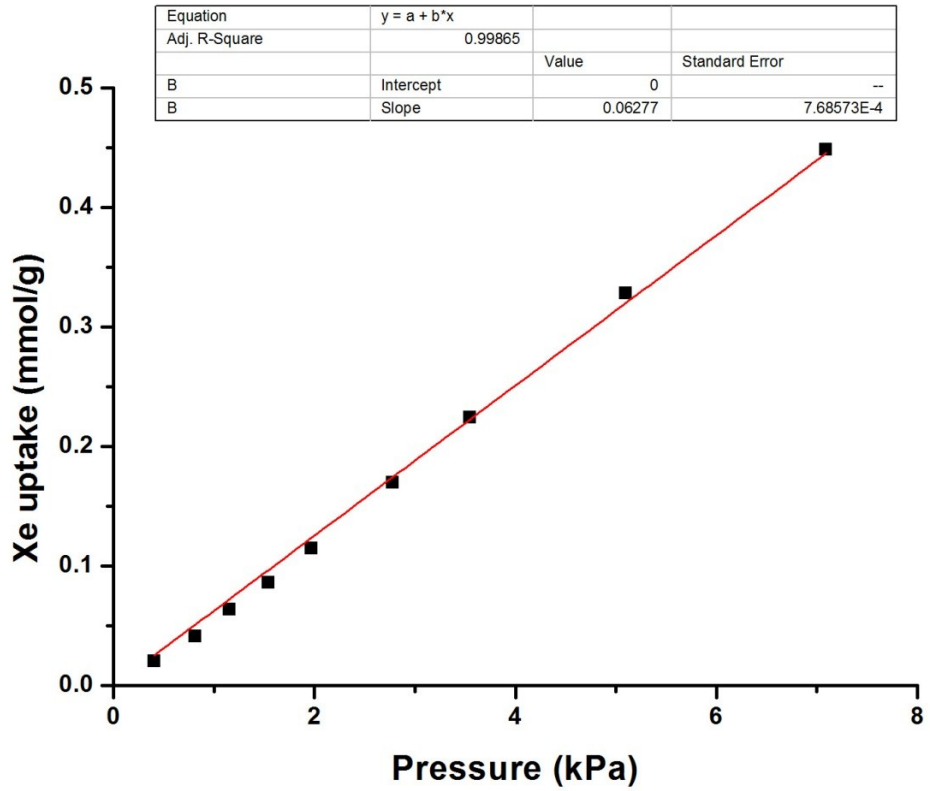

Figure S8. Henry coefficient fitting of Xe adsorption isotherm Co^{2+}-CPM-6 at 298K.

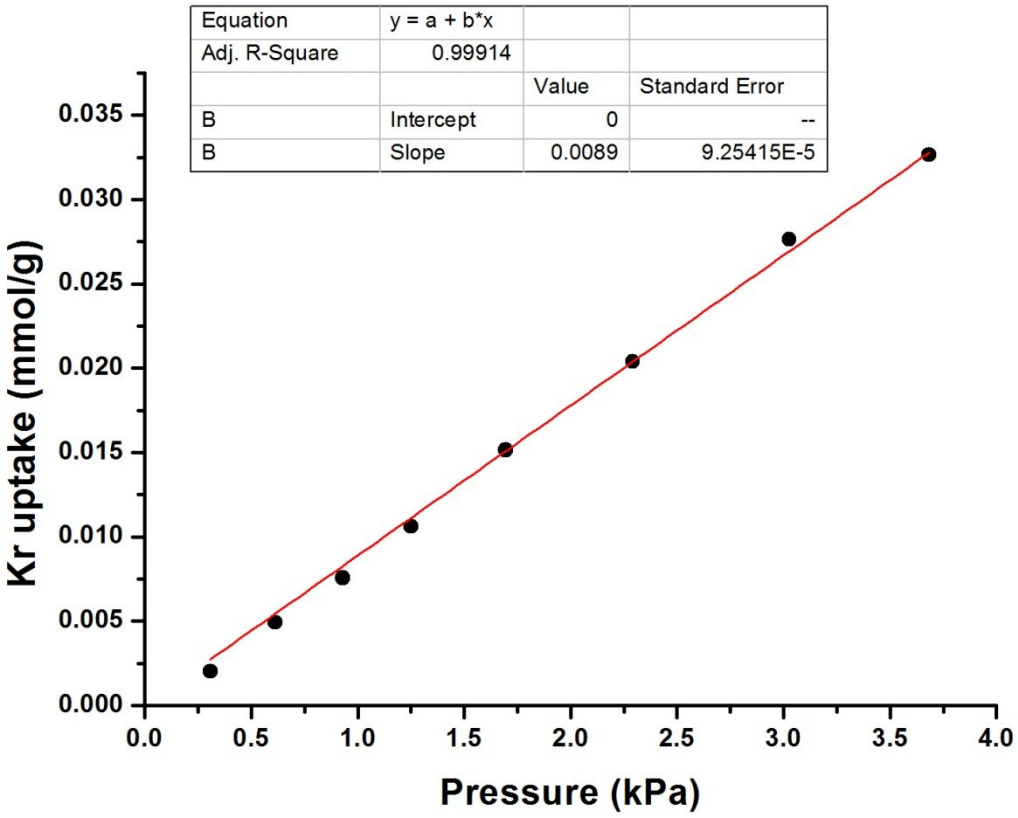

Figure S9. Henry coefficient fitting of Kr adsorption isotherm CPM-5 at 298K.

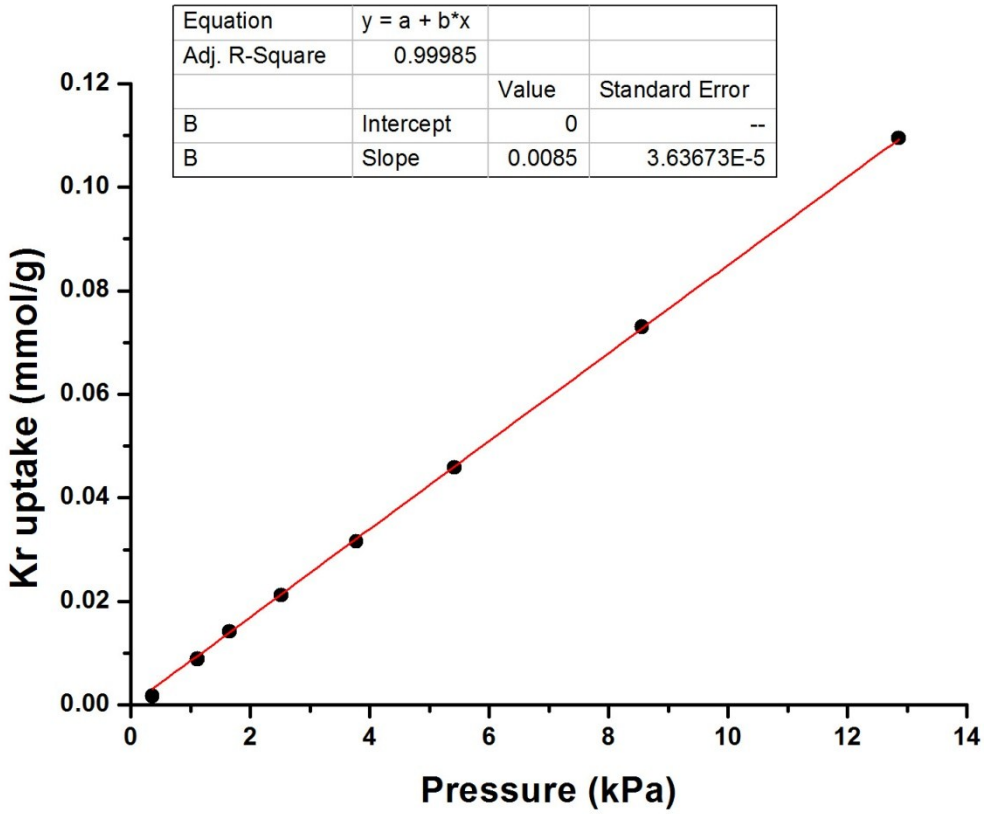

Figure S10. Henry coefficient fitting of Kr adsorption isotherm CPM-6 at 298K.

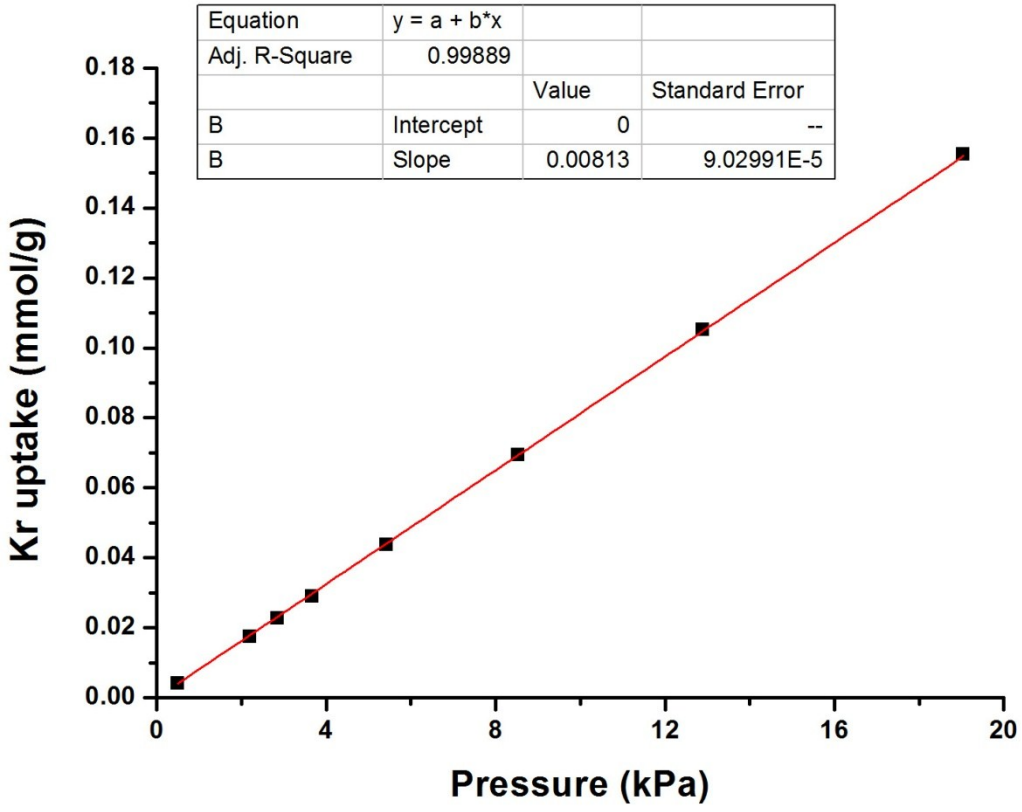

Figure S11. Henry coefficient fitting of Kr adsorption isotherm Co^{2+}-CPM-6 at 298K.

Breakthrough experiments

In a typical breakthrough experiment, about 240~330 mg of MOF samples of CPM-5, CPM-6 and Co^{2+}-CPM-6 were individually packed into three steel columns (the steel column was 20cm long in length with 4 mm of inner (0.64cm outer) diameter with silica wool filling the void space. The adsorbents were heated at 423 K under vacuum conditions for 10 hours and then activated by flowing a helium flow at 323 K for 2 hours before the temperature of the columns were decreased to 298 K. A circulator bath was used to maintain the temperature of the columns at 298 K. The flow of helium gas stream was turned off while a mixture of Xe/Kr (20/80) was sent into the columns. The flow of helium and targeted gas mixture was controlled by two Mass Flow Controllers with flow velocity of 5 ml/min. The downstream was monitored by a Hiden mass spectrometer (HPR 20). Adsorbed amounts of Xe and Kr were calculated by integrating the resulting breakthrough curves by considering dead volume times, which were measured by helium gas under the same flow rate.

The adsorption capacity was estimated from the breakthrough curves using the following equation:

$$n_{adsi} = FC_i t_i \qquad (1)$$

Where n_{adsi} is the adsorption capacity of the gas *i*, *F* is the total molar flow, C_i is the concentration of the gas I entering the column and the ti is the time corresponding to the gas *i*, which is estimated from the breakthrough profile.

The selectivity was then calculated according to the equation:

$$S_{A/B} = \frac{X_A/X_A}{Y_A/Y_B} \qquad (2)$$

Where X_A and X_B are the mole fractions of the gases A and B in the adsorbed phase and Y_A and Y_B are the mole fractions of the gases A and B in the bulk phase.

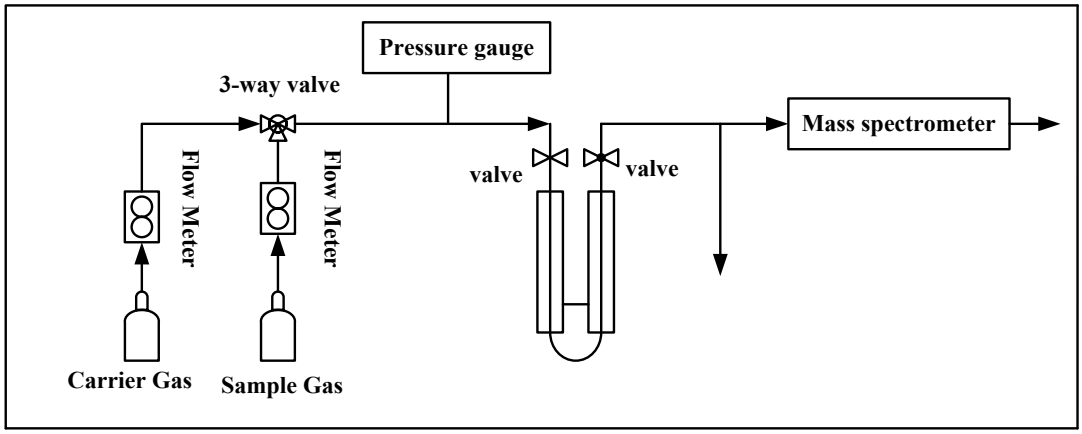

Figure S12. Representation of the dynamic breakthrough experiment.

Dual-site Langmuir- Freundlich Fitting of Pure Component Isotherms

The experimentally measured adsorption isotherms data were fitted using the dual-site Langmuir-Freundlich equation:

$$q = \frac{q_A b_A p^{c_A}}{1 + b_A p^{c_A}} + \frac{q_B b_B p^{c_B}}{1 + b_B p^{c_B}} \quad (1)$$

q_A, q_B are the saturated adsorption amount of noble gas, b_A, b_B are the T-dependent parameters, p is absolute pressure, and c_A, c_B are the fitted parameters.

b_A, b_B can be calculated using the following equation:

$$b_A = b_1 exp(\frac{E_1}{RT}) \quad (2)$$

$$b_B = b_2 exp(\frac{E_2}{RT})$$

Calculation procedures of isoteric adsorption enthalpy

The isosteric enthalpy (Qst) were calculated by the Clausius-Clapeyron equation :

$$\frac{Q_{st}}{R} = \frac{d(lnP)}{d(1/T)} \quad (3)$$

IAST calculation of adsorption selectivity

Ideal Adsorbed Solution Theory (IAST) based on pure component isotherms has been demonstrated to be precise in prediction of selectivity of two components gas mixture at low pressure (0-1bar). The selectivity can be calculated according to the equation:

$$S_{A/B} = \frac{X_A / X_B}{Y_A / Y_B} \quad (4)$$

Where X_A and X_B are the mole fractions of the gases A and B in the adsorbed phase and Y_A and Y_B are the mole fractions of the gases A and B in the bulk phase.

Table S1. Dual-Langmuir-Freundlich parameters for adsorption of Xe and Kr in CPM-5, CPM-6 and Co^{2+}-CPM-6.

	q_1	b_1	c_1	q_2	b_2	c_2	R^2
CPM-5-Xe	1.25	9.87E-4	1.02	2.84	1.9E-3	0.99	0.999
CPM-5-Kr	1.62	6.22E-4	0.988	2.12E-6	8.62E-4	0.79	0.999
CPM-6-Xe	4.25	1.27E-3	1.057	0.08424	1.578E-7	2.8728	0.999

CPM-6-Kr	0.3014	1.3E-3	1.058	23.11	9.08E-6	1.147	0.999
Co-CPM-6-Xe	3.1	0.0148	0.835	2.32	3.9E-3	1.45	0.999
Co-CPM-6-Kr	1.79	4.2E-3	0.97	2.44	1.49E-5	1.68	0.999

Table S2. Xe uptakes and separation in selected porous materials.

Novel porous materials	Specific surface area (m^2/g)	The capacity of Xe (mmol/g)	Xe/Kr selectivity	Xe Qst (kJ/mol)	Ref
IRMOF-1	3400	1.98[1]	3[b]	15	1
Monohalogenated IRMOF-2 series	1900-3100	1.5-2.0[2]	--	11-15	2
Al-MIL-53	1300	2.0[5]	--	--	3
CC3	624	2.69[1]	20.4[a]	31.3	4
NiDOBDC	950	4.19[1]	7.3[a]/5-6[b]	22	5,6
Ag@NiDOBDC	749.7	4.88[1]	6.8[b]	23.6	7
Noria	40	1.55[1]	9.4[b]	24.5-26.9	8
$Co_3(HCOO)_6$	300	2[4]	12[b]	28	9
HKUST-1	1710	3.18[1]	2.6[c]	26.9	10
MFU-4L	3500		4.7(310 K)[d]	20	11
SBMOF-2	195	2.83[1]	10[b]	26.4	12
SBMOF-1	145	1.38[1]	16[a]		13

MOF-505	1030	2.2[4]	9-10[c]		10
FMOFCu	58	~0.45[1]	1[b]	10(>0℃)	14
UTSA-49	710.5	3.0[1]	9.2[b]	23.53 ± 0.54	15
CROFOUR-1-Ni	505[L]	1.8[1]	22[b]/ 19.8[c]	37.4	16
CROFOUR-2-Ni	475[L]	1.6[1]	15.5[b]/14.3[c]	30.5	16
Carbon-ZX	1470	4.42[1]	-	-	17
Co-MOF-74	1346	6.71[3]	10.5[b]/6.4[c]	28.4	18
Mg-MOF-74	1486	~6.5[6]	7[b]	23.5	18
Zn-MOF-74	844	~4.5[6]	7[b]	23.8	18
UiO-66(Zr)	1199	1.58	7.15[d]	25	19
MIL-101(Cr)	3445	1.38	5.33[d]	21.4	19
MIL-100(Fe)	1947	1.14	5.59[d]	20.9	19

a. calculated from breakthrough experiments (298 K 400 ppm Xe, 40 ppm Kr, CO_2, N_2, Ar) b. IAST selectivity c. calculated from breakthrough experiments（298 K 20/80 Xe/Kr mixture）d. calculated from Henry constants L. the surface area calculated by Langmuir method, all the other surface areas are calculated by BET method. 1. 298K, 1bar 2. 292K, 1bar 3. 293K,1bar 4. 298K, 0.2bar 5. 308K, 1bar 6. 283K, 1bar

XPS of Co^{2+}-CPM-6

We performed XPS test for Co^{2+}-CPM-6, and we verified that Co^{2+} was exchanged into the framework by comparing the peak of $2p_{3/2}$ for Co^{2+} in reference 20.

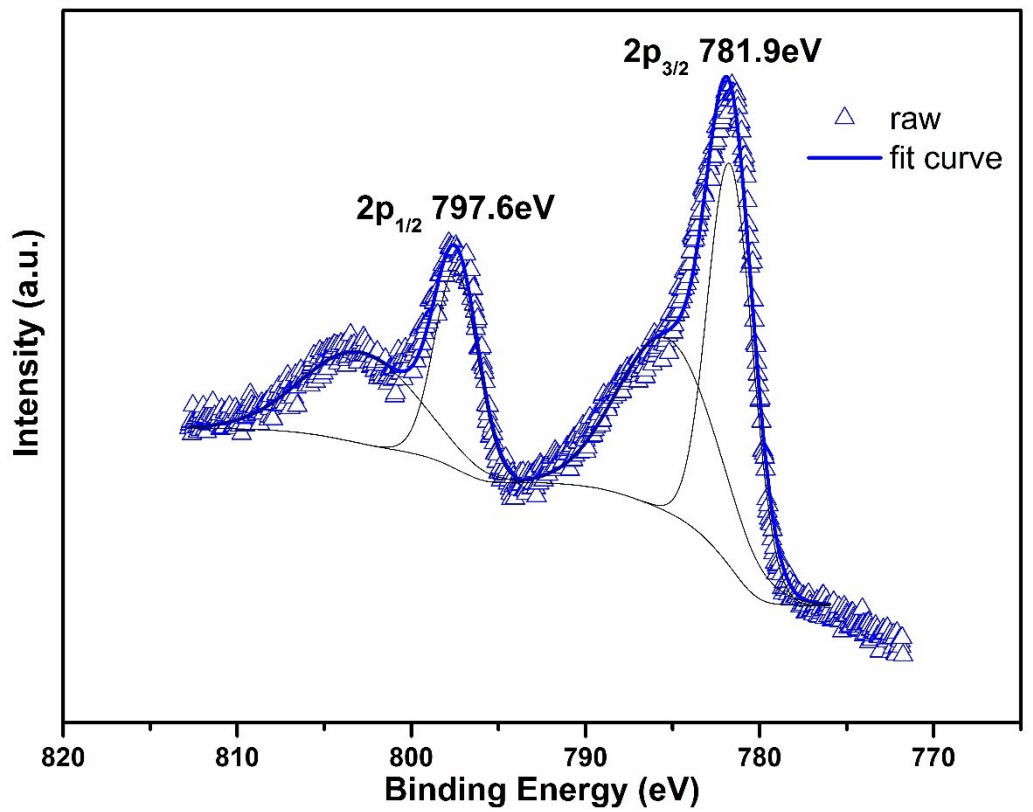

Fig S13. Co 2p spectrum for Co^{2+}-CPM-6

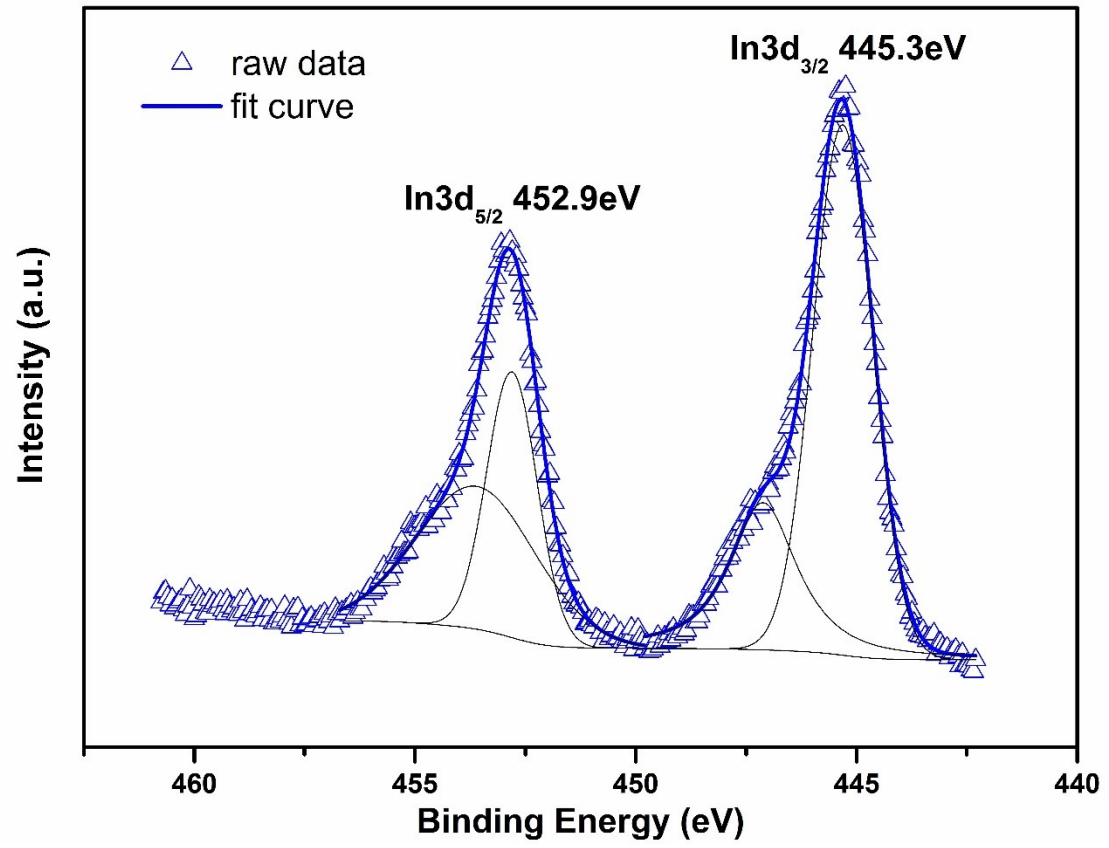

Fig S14. In 3d spectrum for Co^{2+}-CPM-6

Productive rate of CPM-5 and CPM-6

The productive rate of CPM-5 and CPM-6 were about 45% on the base of $In(NO_3)_3 \cdot 5H_2O$

Calculation of ion exchange amount of Co^{2+} in CPM-6

The 62% ion exchange amount was calculated according to the chemical formula of CPM-6: $[CH_3NH_3][In_3O(BTC)_2(H_2O)_3]_2[In_3(BTC)_4] \cdot$ solvent. 1mg Co^{2+}-CPM-6 was dissolved in concentrated HCl and diluted to 100ml to prepare the test sample with the concentration of 10ppm. And external standard method was adopted in this test. We prepared standard solutions with the concentration of 1ppm, 5ppm, 10ppm to obtain calibration curve, then the sample was tested on the basis of that curve. According to the chemical formula of CPM-6, the molar ratio of In/$[CH_3NH_3]^+$ is 9, if Co^{2+} is utterly exchanged into the framework, the molar ratio of In/Co is supposed to be 18. But the test result is 29, thus the ion exchange amount is supposed to be $18/29 \times 100\% = 62\%$

Abbreviation list

NiDOBDC is also called MOF-74Ni, is a kind of nickel-based MOF and DOBDC is abbreviation of 2,5-dihydroxyterephthalic acid

Co-MOF-74 has the same structure with NiDOBDC except the central metal atom is Co

Ag@MOF-74Ni is Ag loaded MOF-74Ni

CC3 is a kind of porous organic cage, its molecular formula is $C_{72}H_{85}N_{12}$.

Hmtz is abbreviation of 5-methyl-1H-tetrazole

SBMOF-1 is also known as CaSDB, SDB=4,4 –sulfonyldibenzoate

SBMOF-2 is abbreviation of Stony Brook MOF-2

BTC is abbreviation of 1,3,5-Benzenetricarboxylic acid

DMF is abbreviation of N,N-dimethyllformamide

NMF is abbreviation of Methyl Formamide

Reference

[1] U. Mueller, M. Schubert, F. Teich, H. Puetter, K. Schierle-Arndt and J. Pastre, *Journal of Materials Chemistry*, 2006, **16**, 626-636.

[2] S. T. Meek, S. L. Teich-McGoldrick, J. J. Perry, J. A. Greathouse and M. D. Allendorf, *The Journal of Physical Chemistry C*, 2012, **116**, 19765-19772.

[3] A. Boutin, M. A. Springuel-Huet, A. Nossov, A. Gédéon, T. Loiseau, C. Volkringer, G. Férey, F. X. Coudert and A. H. Fuchs, *Angewandte Chemie International Edition*, 2009, **48**, 8314.

[4] L Chen, P. S. Reiss, S. Y. Chong, D. Holden, K. E. Jelfs, T. Hasell, M. A. Little, A. Kewley, M. E. Briggs, A. Stephenson, K. M. Thomas, J. A. Armstrong, J. Bell, J. Busto, R. Noel, J. Liu, D. M. Strachan, P. K. Thallapally and A. I. Cooper, *Nature materials*, 2014, **13**, 954.

[5] P. K. Thallapally, J. W. Grate and R. K. Motkuri, *Chemical Communications*, 2012, **48**, 347.

[6] J. Liu, P. K. Thallapally and D. M. Strachan, *Langmuir*, 2012, **28**, 11584.
[7] J. Liu, D. M. Strachan and P. K. Thallapally, *Chemical Communications*, 2014, **50**, 466.
[8] R. S. Patil, D. Banerjee, C. M. Simon, J. L. Atwood and P. K. Thallapally, *Chemistry-A European Journal*, 2016, **22**, 12618.
[9] H. Wang, K. Yao, Z. Zhang, J. Jagiello, Q. Gong, Y. Han and J. Li, *Chemical Science*, 2014, **5**, 620.
[10] Y.-S. Bae, B. G. Hauser, Y. J. Colón, J. T. Hupp, O. K. Farha and R. Q. Snurr, *Microporous and Mesoporous Materials*, 2013, **169**, 176.
[11] A. S. Dorcheh, D. Denysenko, D. Volkmer, W. Donner and M. Hirscher, *Microporous and Mesoporous Materials*, 2012, **162***,* 64.
[12] X. Chen, A. M. Plonka, D. Banerjee, R. Krishna, H. T. Schaef, S. Ghose, P. K. Thallapally, and J. B. Parise, *Journal of the American Chemical Society,* 2015, **137**, 7007.
[13] D. Banerjee, C. M. Simon, A. M. Plonka, R. K. Motkuri, J. Liu, X. Chen, B. Smit, J. B. Parise, M. Haranczyk and P. K. Thallapally, *Nature communications*, 2016, **7**.
[14] C. A. Fernandez, J. Liu, P. K. Thallapally and D. M. Strachan, *Journal of the American Chemical Society*, 2012, **134**, 9046.
[15] S. Xiong, Q. Liu, Q. Wang, W. Li, Y. Tang, X. Wang, S. Hu and B. Chen, *Journal of Materials Chemistry A*, 2015, **3**, 10747.
[16] M. H. Mohamed, S. K. Elsaidi, T. Pham, K. A. Forrest, H. T. Schaef, A. Hogan, L. Wojtas, W. Xu, B. Space, M. J. Zaworotko and P. K. Thallapally, *Angewandte Chemie International Edition*, 2016, **55**, 8285.
[17] S. Zhong, Q Wang, D Cao. *Scientific reports*, 2016, **6**.
[18] S.-J. Lee, K. C. Kim, T.-U. Yoon, M.-B. Kim, Y.-S. Bae, *Microporous and Mesoporous Materials*, 2016, **236**, 284-291.
[19] S.-J. Lee, T.-U. Yoon, A.-R. Kim, S.-Y. Kim, K.-H. Cho, Y. K. Hwang, J.-W. Yeon, Y.-S. Bae, *Journal of Hazardous Materials*, 2016, **320**, 513-520.
[20] Z. Zsoldos, G. Vass, G. Lu, L. Guczi. *Applied Surface Science,* 1994, **78**, 467-475.